

CP violation in charged Higgs decays in the MSSM

Ekaterina Christova[†], Helmut Eberl[‡], Elena Ginina[†], Walter Majerotto[‡]

[†]*Institute of Nuclear Research and Nuclear Energy, Sofia 1784, Bulgaria*

[‡]*Institut für Hochenergiephysik der Österreichischen Akademie der Wissenschaften,
A-1050 Vienna, Austria*

E-mails: `echristo@inrne.bas.bg`, `helmut@hephy.oeaw.ac.at`,
`eginina@inrne.bas.bg`, `majer@hephy.oeaw.ac.at`

ABSTRACT: In the MSSM with complex parameters loop corrections to the decays $H^+ \rightarrow t \bar{b}$ and $H^- \rightarrow \bar{t} b$ with $t \rightarrow b W$ and $W \rightarrow l \nu$ lead to CP-violating asymmetries: a decay rate asymmetry, a forward-backward asymmetry and an energy asymmetry. We derive explicit formulas for them and perform a detailed numerical analysis. We study the dependence on the parameters and the phases involved. In particular, the influence of the running Yukawa coupling is taken into account. The decay rate asymmetry can go up to 25%, the forward-backward and the energy asymmetry up to 10%.

KEYWORDS: Supersymmetric Standard Model, Higgs Physics, CP violation.

Contents

1. Introduction	1
2. Formalism	3
2.1 The t-quark polarization vector	4
2.2 CP-violating asymmetries	4
3. The $H^\pm \rightarrow W^\pm bb'$ process	5
3.1 Angular distributions	5
3.2 Energy distributions	6
4. The $H^\pm \rightarrow bb'l^\pm\nu$ process	7
5. Numerical Results	8
5.1 The CP-violating asymmetries	8
5.2 The P-violating asymmetries	11
6. Conclusions	12
A. Running Yukawa couplings	15
B. Squark–quark–gluino contribution	16

1. Introduction

It is well known that supersymmetric models contain new sources of CP violation if the parameters are complex. In the Minimal Supersymmetric Standard Model (MSSM) the U(1) and SU(2) gaugino mass parameters M_1 and M_2 , the higgsino mass parameter μ , as well as the trilinear couplings A_f (corresponding to a fermion f) may be complex. (Usually, M_2 is made real by redefining the fields.) Non-vanishing phases of these parameters cause CP-violating effects. While the phase of μ may be small for a supersymmetric particle spectrum of $\mathcal{O}(100 \text{ GeV})$ due to the experimental upper bounds of the electric dipole moments (EDMs) of electron and neutron, the trilinear couplings of the third generation $A_{t,b,\tau}$ are not so much constrained and can lead to significant CP-violation [1, 2].

In the following, we study CP violation in the decays of the charged Higgs bosons H^\pm within the MSSM. There are three possible decays of H^\pm into ordinary particles: H^+ into $t\bar{b}$, $\tau\nu$ and Wh^0 and the CP conjugated ones, where h^0 is the lightest neutral Higgs boson of the MSSM. At tree level the partial decay widths of H^+ and H^- are equal because of CP invariance of the Higgs potential. However, including loop corrections with intermediate SUSY-particles, they become different due to the CP violation induced by the complex

phases of the MSSM parameters, essentially of $A_{t,b,\tau}$. Quite generally, these phases affect the whole Higgs sector of the MSSM substantially [3, 4].

A full one-loop calculation within the MSSM was done of the decays mentioned [5, 6, 7, 8], and the CP-violating decay rate asymmetry $\delta^{CP} = [\Gamma_{H^+} - \Gamma_{H^-}]/[\Gamma_{H^+} + \Gamma_{H^-}]$ for these decays was calculated. In the case of $H^+ \rightarrow \bar{b}t$ and $H^- \rightarrow \bar{b}t$ this asymmetry can go up to $\sim 25\%$.

In this paper, we go a step further by including the decay product particles of the top quark, see Fig. 1,

$$\begin{aligned} H^+ &\rightarrow \bar{b}t \rightarrow \bar{b}b'W^+, \\ H^- &\rightarrow b\bar{t} \rightarrow b\bar{b}'W^-, \end{aligned} \quad (1.1)$$

and

$$\begin{aligned} H^+ &\rightarrow \bar{b}t \rightarrow \bar{b}b'W^+ \rightarrow \bar{b}b'l^+\nu_l, \\ H^- &\rightarrow b\bar{t} \rightarrow b\bar{b}'W^- \rightarrow b\bar{b}l^-\bar{\nu}_l. \end{aligned} \quad (1.2)$$

We only consider CP violation induced by the loop diagrams of $H^\pm tb$ vertex. We neglect CP violation in the tWb' vertex. In the Standard model it is very small and in the MSSM for $m_{H^+} > m_t$ all two-body decays of top into SUSY partners are excluded kinematically.

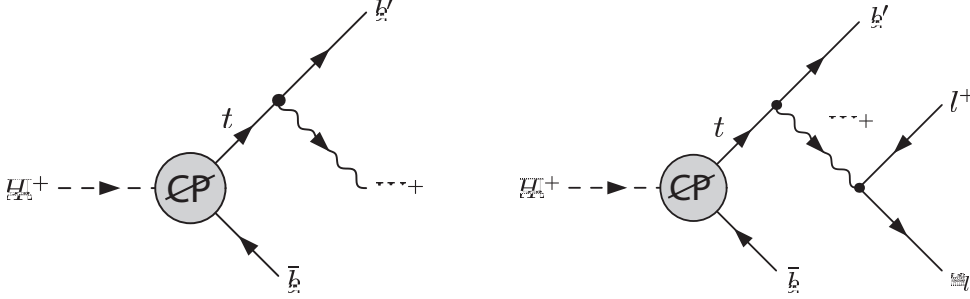


Figure 1: The Feynman graphs of the processes we study.

In particular, we will exploit the polarization of the top quark. The top-quark decays before forming a bound state due to its large mass, so that the polarization can be measured by the angular distributions of its decay products. The polarization is very sensitive to CP violation. We will consider suitable CP violating forward-backward and energy asymmetries by using angular or energy distributions of the decay particles. The asymmetries also depend on the sensitivity of b' in (1.1) or the final lepton l^\pm in (1.2) to the top-quark polarization. Further we make a numerical analysis for different values of the MSSM parameters.

This paper is organized in the following order. In Section 2 we present the formalism we use. There are subsections devoted to the polarization of the top quark and the CP-violating asymmetries. Sections 3 and 4 contain the angular and energy distributions and the analytic results for the asymmetries of (1.1) and (1.2), respectively. The numerical results are discussed in Section 5. Section 6 contains the conclusions. In Appendix A the formulas used for running Yukawa couplings h_b and h_t are given. In Appendix B we point out an error made in an equation of [5].

2. Formalism

In order to obtain the analytic expressions for the differential partial decay rates of (1.1) and (1.2), we follow the formalism of [9]. In accordance with it, for both of the processes we write

$$d\Gamma_f^\pm = d\Gamma_{H^\pm} d\Gamma_{t,\bar{t}}^f \frac{E_{t,\bar{t}}}{m_t \Gamma_t}, \quad f = b', l. \quad (2.1)$$

$E_{t,\bar{t}}$ is the energy of $t(\bar{t})$ -quark, and Γ_t is the total decay width of the t -quark. $d\Gamma_{H^\pm}$ is the differential partial decay rate of the process $H^\pm \rightarrow tb$ when CP-violation is included:

$$d\Gamma_{H^\pm} = \frac{1}{2m_H} |\mathcal{M}_{H^\pm}|^2 d\Phi_{H^\pm}. \quad (2.2)$$

where $d\Phi_{H^\pm}$ is the relevant phase space element and

$$\mathcal{M}_{H^+} = i\bar{u}(p_t)[Y_b^+ P_R + Y_t^+ P_L]u(-p_b), \quad (2.3)$$

$$\mathcal{M}_{H^-} = i\bar{u}(p_b)[Y_t^- P_R + Y_b^- P_L]u(-p_{\bar{t}}), \quad (2.4)$$

$$Y_t^\pm = y_t + \delta Y_t^\pm, \quad Y_b^\pm = y_b + \delta Y_b^\pm. \quad (2.5)$$

Here y_t and y_b are the $\overline{\text{DR}}$ running couplings, see Appendix A, $\delta Y_{t,b}^\pm$ are the SUSY-induced loop corrections, which most generally have CP-invariant and CP-violating parts:

$$\delta Y_{t,b}^\pm = \delta Y_{t,b}^{inv} \pm \frac{1}{2} \delta Y_{t,b}^{CP}. \quad (2.6)$$

$d\Gamma_{t,\bar{t}}^f$ is the differential partial rate of the process $t \rightarrow b'W^\pm$ or $t \rightarrow b'l^\pm\nu$ when the t -quark is polarized and its polarization is determined in the former process $H^\pm \rightarrow t\bar{b}$:

$$d\Gamma_{t,\bar{t}}^f = \Gamma_f^0 \left[1 \pm \alpha_f m_t \frac{(\xi_{t,\bar{t}} p_f)}{(p_t p_f)} \right] d\Phi_{t,\bar{t}}^f. \quad (2.7)$$

ξ_t^α is the polarization vector of the t -quark and $d\Phi_{t,\bar{t}}^f$ are the phase space elements. The index f stands for the corresponding fermion ($f = b', l$) and α_f determines its sensitivity to the polarization of the t -quark:

$$\alpha_b = \frac{m_t^2 - 2m_W^2}{m_t^2 + 2m_W^2}, \quad \alpha_l = 1. \quad (2.8)$$

In the kinematics of both of the processes (1.1) and (1.2) we work in the approximation

$$m_l^2/m_W^2 \simeq m_b^2/m_t^2 \simeq m_b^2/m_W^2 \simeq 0, \quad (2.9)$$

but we keep $m_b \neq 0$ in the couplings, where it is multiplied by $\tan\beta$.

2.1 The t-quark polarization vector

The polarization four-vectors ξ_t^α and $\xi_{\bar{t}}^\alpha$ for the considered processes are covariantly given by the expressions [9]:

$$\xi_t^\alpha = \left(g^{\alpha\beta} - \frac{p_t^\alpha p_t^\beta}{m_t^2} \right) \frac{\text{Tr}[M_{H^+}(-\Lambda(-p_{\bar{b}}))\overline{M}_{H^+}\Lambda(p_t)\gamma_\beta\gamma_5]}{\text{Tr}[M_{H^+}(-1)\Lambda(-p_{\bar{b}})\overline{M}_{H^+}\Lambda(p_t)]}, \quad (2.10)$$

$$\xi_{\bar{t}}^\alpha = \left(g^{\alpha\beta} - \frac{p_{\bar{t}}^\alpha p_{\bar{t}}^\beta}{m_t^2} \right) \frac{\text{Tr}[M_{H^-}(-\Lambda(-p_{\bar{t}}))\overline{M}_{H^-}\Lambda(p_b)\gamma_\beta\gamma_5]}{\text{Tr}[M_{H^-}(-1)\Lambda(-p_{\bar{t}})\overline{M}_{H^-}\Lambda(p_b)]}, \quad (2.11)$$

where

$$M_{H^+} = Y_b^+ P_R + Y_t^+ P_L, \quad M_{H^-} = Y_t^- P_R + Y_b^- P_L, \quad (2.12)$$

$$\overline{M} = \gamma_0 M^\dagger \gamma_0, \quad \Lambda(p_t) = \not{p}_t + m_t. \quad (2.13)$$

Thus we obtain:

$$\xi_{t,\bar{t}}^\alpha = m_t \mathcal{P}^\pm Q_{b,\bar{b}}^\alpha, \quad Q_{b,\bar{b}}^\alpha = p_{b,\bar{b}}^\alpha - \frac{(p_t p_{\bar{b}})}{m_t^2} p_{t,\bar{t}}^\alpha. \quad (2.14)$$

Notice that the four-vector $Q_{b,\bar{b}}^\alpha$ is the only four-vector in $H^\pm \rightarrow tb$ that can be constructed so that it satisfies the orthogonal condition $(\xi_t p_t) = 0$. The polarization vectors (2.14) have CP-invariant and CP-violating parts, and the CP-violating parts are only due to the loop corrections:

$$\mathcal{P}^\pm = \pm \mathcal{P}^{inv} + \mathcal{P}^{CP}, \quad (2.15)$$

$$\mathcal{P}^{inv} = \frac{y_t^2 - y_b^2}{(y_t^2 + y_b^2)(p_t p_{\bar{b}}) - 2m_t m_b y_t y_b}, \quad (2.16)$$

$$\mathcal{P}^{CP} = \frac{y_t \text{Re}(\delta Y_t^{CP}) - y_b \text{Re}(\delta Y_b^{CP})}{(y_t^2 + y_b^2)(p_t p_{\bar{b}}) - 2m_t m_b y_t y_b}. \quad (2.17)$$

The explicit forms of the individual contributions to $\text{Re}(\delta Y_{t,b}^{CP})$ are taken from [5].

2.2 CP-violating asymmetries

The CP-violating decay rate asymmetry δ^{CP} is given by the expression

$$\delta^{CP} = \frac{\Gamma_+ - \Gamma_-}{\Gamma_+ + \Gamma_-}. \quad (2.18)$$

In (2.18) Γ_\pm are the partial decay widths of H^\pm .

Next, we construct a CP-violating forward-backward (FB) asymmetry ΔA^{CP} from the FB asymmetries A_\pm^{FB} using the angular distributions of the processes

$$\Delta A^{CP} = A_+^{FB} - A_-^{FB}, \quad (2.19)$$

where

$$A_\pm^{FB} = \frac{\Gamma_\pm^F - \Gamma_\pm^B}{\Gamma_\pm^F + \Gamma_\pm^B}, \quad (2.20)$$

$$\Gamma_\pm^F = \int_0^{\frac{\pi}{2}} \frac{d\Gamma^\pm}{d\cos\theta} d\cos\theta \quad \text{and} \quad \Gamma_\pm^B = \int_{\frac{\pi}{2}}^\pi \frac{d\Gamma^\pm}{d\cos\theta} d\cos\theta, \quad (2.21)$$

i.e. Γ_{\pm}^F are the number of particles /antiparticles measured in the forward direction of the decaying t/\bar{t} quarks, etc.

Analogously, a CP-violating energy asymmetry ΔR^{CP} can be defined, using the energy distributions of the processes

$$\Delta R^{CP} = R_+ - R_- , \quad (2.22)$$

where R_{\pm} are

$$R_{\pm} = \frac{\Gamma_{\pm}(x > x_0) - \Gamma_{\pm}(x < x_0)}{\Gamma_{\pm}(x > x_0) + \Gamma_{\pm}(x < x_0)} . \quad (2.23)$$

x is a dimensionless variable proportional to the energy, and x_0 is any fixed value in the energy interval.

3. The $H^{\pm} \rightarrow W^{\pm}bb'$ process

Following the formalism of Section 2 for the differential partial decay rate of the process (1.1) in the rest frame of H^{\pm} , we obtain

$$d\Gamma_b^{\pm} = \Gamma_{H^{\pm}} \Gamma_b^0 \left[1 \pm \alpha_b m_t \frac{(\xi_{t,\bar{t}} p_{b'}, \bar{b}')}{(p_t p_{\bar{b}})} \right] \frac{E_{t,\bar{t}}}{m_t \Gamma_t} d\Phi_{b',\bar{b}'} . \quad (3.1)$$

$\Gamma_{H^{\pm}}$ is the partial decay width of the process $H^{\pm} \rightarrow tb$, assuming CP-violation in its vertex

$$\Gamma_{H^{\pm}} = \mathcal{C}_H (\Gamma^{inv} \pm \Gamma^{CP}) , \quad (3.2)$$

where

$$\mathcal{C}_H = \frac{3\alpha_{\omega} \lambda^{1/2}(m_H^2, m_t^2, m_b^2)}{4m_H^3 m_W^2}, \quad \alpha_{\omega} = \frac{g^2}{4\pi}, \quad (3.3)$$

$$\Gamma^{inv} = (y_t^2 + y_b^2)(p_t p_{\bar{b}}) - 2m_t m_b y_t y_b , \quad (3.4)$$

$$\Gamma^{CP} = [y_t \text{Re}(\delta Y_t^{CP}) + (y_b \text{Re}(\delta Y_b^{CP}))](p_t p_{\bar{b}}) - m_t m_b [y_t \text{Re}(\delta Y_b^{CP}) + y_b \text{Re}(\delta Y_t^{CP})] , \quad (3.5)$$

$$\lambda(x, y, z) = x^2 + y^2 + z^2 - 2xy - 2xz - 2yz, \quad \lambda^{1/2}(m_H^2, m_t^2, m_b^2) \approx m_H^2 - m_t^2, \quad (3.6)$$

$$(p_t p_{\bar{b}}) = \frac{1}{2}(m_H^2 - m_t^2 - m_b^2) \simeq \frac{1}{2}(m_H^2 - m_t^2), \quad (3.7)$$

$$\Gamma_b^0 = \frac{g^2(m_t^2 - m_W^2)(m_t^2 + 2m_W^2)}{8m_W^2 E_t}, \quad \text{and} \quad d\Phi_{b',\bar{b}'} = -\frac{(m_t^2 - m_W^2) d \cos \theta_{b',\bar{b}'}}{16\pi E_t^2 (1 - \beta_t \cos \theta_{b',\bar{b}'})^2}. \quad (3.8)$$

3.1 Angular distributions

For the angular distributions of $b'(\bar{b}')$ when the 3-momentum of the $t(\bar{t})$ -quark is along the z-axis one gets

$$\begin{aligned} \frac{d\Gamma_b^{\pm}}{d \cos \theta_{b',\bar{b}'}} &= \frac{\mathcal{C}_b}{(1 - \beta_t \cos \theta_{b',\bar{b}'})^2} \left\{ \Gamma^{inv} \pm \Gamma^{CP} + \right. \\ &\quad \left. \alpha_b m_t^2 [\Gamma^{inv} \mathcal{P}^{inv} \pm (\Gamma^{CP} \mathcal{P}^{inv} + \Gamma^{inv} \mathcal{P}^{CP})] \left(\frac{E_{\bar{b}}(1 + \cos \theta_{b',\bar{b}'})}{E_t(1 - \beta_t \cos \theta_{b',\bar{b}'})} - \frac{(p_t p_{\bar{b}})}{m_t^2} \right) \right\} , \end{aligned} \quad (3.9)$$

where

$$C_b = -\frac{3\alpha_\omega^2 |\vec{p}_t| (m_t^2 - m_W^2)^2 (m_t^2 + 2m_W^2)}{64m_H^2 m_W^4 E_t^2 m_t \Gamma_t}, \quad (3.10)$$

$$\beta_t = \frac{|\vec{p}_t|}{E_t}, \quad |\vec{p}_t| = \frac{\lambda^{1/2}(m_H^2, m_t^2, m_b^2)}{2m_H} \simeq \frac{m_H^2 - m_t^2}{2m_H}, \quad (3.11)$$

$$E_t = \frac{m_H^2 + m_t^2 - m_b^2}{2m_H} \simeq \frac{m_H^2 + m_t^2}{2m_H}, \quad E_{\bar{b}} = \frac{m_H^2 + m_b^2 - m_t^2}{2m_H} \simeq \frac{m_H^2 - m_t^2}{2m_H}. \quad (3.12)$$

We are interested in the CP-violating contributions to the loop corrections of the $H^\pm b t$ vertex (2.6). The quantities δY_t^{CP} and δY_b^{CP} enter the two independent combinations Γ^{CP} and \mathcal{P}^{CP} . One therefore needs two measurements to determine them. The decay rate asymmetry δ_b^{CP} for process (1.1) measures Γ^{CP} given in (3.5),

$$\delta_b^{CP} = \frac{N_{b'} - N_{\bar{b}'}}{N_{b'} + N_{\bar{b}'}} = \frac{\Gamma^{CP}}{\Gamma^{inv}}, \quad (3.13)$$

where $N_{b'}(\bar{b}')$ are the total number of b' (\bar{b}') in $H^\pm \rightarrow b b' W^\pm$ decay.

The CP-violating angular asymmetry ΔA^{CP} measures the other combination \mathcal{P}^{CP} given in (2.17). We have

$$\Delta A_b^{CP} = 2\alpha_b m_t^2 m_H^2 \frac{m_H^2 - m_t^2}{(m_H^2 + m_t^2)^2} \mathcal{P}^{CP} \quad (3.14)$$

The FB asymmetries are given by

$$A_{b\pm}^{FB} = \beta_t + \alpha_b m_t^2 m_H^2 \frac{(m_H^2 - m_t^2)}{(m_H^2 + m_t^2)^2} \frac{(\Gamma^{inv} \mathcal{P}^{inv} \pm \Gamma^{CP} \mathcal{P}^{inv} \pm \Gamma^{inv} \mathcal{P}^{CP})}{\Gamma^{inv} \pm \Gamma^{CP}}. \quad (3.15)$$

Using the expansion

$$\frac{(\Gamma^{inv} \mathcal{P}^{inv} \pm \Gamma^{CP} \mathcal{P}^{inv} \pm \Gamma^{inv} \mathcal{P}^{CP})}{\Gamma^{inv} \pm \Gamma^{CP}} = \mathcal{P}^{inv} \pm \mathcal{P}^{CP} + \text{higher orders}, \quad (3.16)$$

we get at one-loop level

$$A_{b\pm}^{FB} = \beta_t + \alpha_b m_t^2 m_H^2 \frac{(m_H^2 - m_t^2)}{(m_H^2 + m_t^2)^2} (\mathcal{P}^{inv} \pm \mathcal{P}^{CP}). \quad (3.17)$$

3.2 Energy distributions

We write the energy distribution of $b'(\bar{b}')$ as a function of $x = E_{b'}/m_H$ ($x = E_{\bar{b}'}/m_H$):

$$\frac{d\Gamma^\pm}{dx} = C_E [c_0^\pm + c_1^\pm x], \quad (3.18)$$

where

$$C_E = \frac{3\alpha_\omega^2 (m_t^2 - m_W^2)(m_t^2 + 2m_W^2)}{2^6 m_W^4 m_H^2 m_t \Gamma_t}, \quad c_0^\pm = c_0^{inv} \pm c_0^{CP}, \quad c_1^\pm = c_1^{inv} \pm c_1^{CP}, \quad (3.19)$$

$$c_0^{inv} = \Gamma^{inv} - \alpha_b \frac{(m_H^2 + m_t^2)}{2} \Gamma^{inv} \mathcal{P}^{inv}, \quad (3.20)$$

$$c_0^{CP} = \Gamma^{CP} - \alpha_b \frac{(m_H^2 + m_t^2)}{2} (\Gamma^{inv} \mathcal{P}^{CP} + \Gamma^{CP} \mathcal{P}^{inv}), \quad (3.21)$$

$$c_1^{inv} = 2\alpha_b \frac{m_H^2 m_t^2}{(m_t^2 - m_W^2)} \Gamma^{inv} \mathcal{P}^{inv}, \quad c_1^{CP} = 2\alpha_b \frac{m_H^2 m_t^2}{(m_t^2 - m_W^2)} (\Gamma^{inv} \mathcal{P}^{CP} + \Gamma^{CP} \mathcal{P}^{inv}). \quad (3.22)$$

The asymmetry ΔR^{CP} also measures \mathcal{P}^{CP} . We choose $x_0 = (x_{min} + x_{max})/2$. Inserting the one-loop result

$$R_{b\pm} = \frac{1}{4} \alpha_b (m_H^2 - m_t^2) (\mathcal{P}^{inv} \pm \mathcal{P}^{CP}) \quad (3.23)$$

into eq.(2.23) gives

$$\Delta R_b^{CP} = \frac{1}{2} \alpha_b (m_H^2 - m_t^2) \mathcal{P}^{CP}. \quad (3.24)$$

4. The $H^\pm \rightarrow bb'l^\pm \nu$ process

In order to obtain the differential partial decay rate of (1.2), we fix the coordinate system such that the t-quark points in the direction of the z-axis and the 3-momenta of t and l determine the yz-plane:

$$\begin{aligned} \vec{p}_{t,\bar{t}} &= |\vec{p}_{t,\bar{t}}| (0, 0, 1), & \vec{p}_{l^\pm} &= |\vec{p}_{l^\pm}| (0, \sin \theta_{l^\pm}, \cos \theta_{l^\pm}), \\ \vec{p}_{b',\bar{b}'} &= |\vec{p}_{b',\bar{b}'}| (\sin \theta_{b',\bar{b}'} \cos \phi_{b',\bar{b}'}, \sin \theta_{b',\bar{b}'} \sin \phi_{b',\bar{b}'}, \cos \theta_{b',\bar{b}'}). \end{aligned} \quad (4.1)$$

The angular distributions of l^\pm are then given by

$$d\Gamma_l^\pm = \Gamma_H^\pm \Gamma_l^0 \left[1 \pm \alpha_l m_t \frac{(\xi_{t,\bar{t}} p_{l^\pm})}{(p_t p_l)} \right] \frac{E_{t,\bar{t}}}{m_t \Gamma_t} d\Phi_{l^\pm}, \quad (4.2)$$

where

$$\Gamma_l^0 = \frac{g^4 \pi [m_t^2 - 2(p_t p_l)] (p_t p_l)}{2 E_t m_W \Gamma_W}, \quad \delta(p_W^2 - m_W^2) d\Phi_{l^\pm} = \frac{1}{(2\pi)^4} \frac{E_{b'}^2 E_l^2 d\Omega_{b'} d\cos \theta_l}{4(m_t^2 - m_W^2) m_W^2}, \quad (4.3)$$

$$(p_t p_l) = E_t E_l (1 - \beta_t \cos \theta_l), \quad (4.4)$$

$$E_l = \frac{m_W^2}{2[E_t(1 - \beta_t \cos \theta_l) - E_{b'}(1 - \cos \theta_{lb'})]} \quad \text{and} \quad E_{b'} = \frac{m_t^2 - m_W^2}{2E_t(1 - \beta_t \cos \theta_{b'})}. \quad (4.5)$$

The angle $\theta_{lb'}$ is between \vec{p}_l and $\vec{p}_{b'}$:

$$\cos \theta_{lb'} = \sin \theta_l \sin \theta_{b'} \sin \phi_{b'} + \cos \theta_l \cos \theta_{b'}. \quad (4.6)$$

The angular distributions of l^\pm then reads

$$\begin{aligned} \frac{d\Gamma_l^\pm}{d\cos \theta_{l^\pm}} &= \frac{\mathcal{C}_l}{(1 - \beta_t \cos \theta_{l^\pm})^2} \left\{ \Gamma^{inv} \pm \Gamma^{CP} + \right. \\ &\quad \left. \alpha_l m_t^2 [\Gamma^{inv} \mathcal{P}^{inv} \pm (\Gamma^{inv} \mathcal{P}^{CP} + \Gamma^{CP} \mathcal{P}^{inv})] \left(\frac{E_{\bar{b}}(1 + \cos \theta_{l^\pm})}{E_t(1 - \beta_t \cos \theta_{l^\pm})} - \frac{(p_t p_{\bar{b}})}{m_t^2} \right) \right\}, \end{aligned} \quad (4.7)$$

where

$$\mathcal{C}_l = -\alpha_\omega^3 m_W |\vec{p}_t| (m_t^2 - m_W^2)^2 \times \frac{[6(1 - \beta_t^2)^2 E_t^4 + 3m_t^4 - 5m_t^2 m_W^2 + 2m_W^4 - 3(1 - \beta_t^2) E_t^2 (3m_t^2 - 2m_W^2)]}{2^8 m_H^2 m_t \Gamma_t \Gamma_W E_t^2 [m_t^2 - m_W^2 - (1 - \beta_t^2) E_t^2]^3}. \quad (4.8)$$

Γ_W is the total decay width of the W boson.

As there is no CP violation in $t \rightarrow bl\nu$ decay, the decay rate asymmetry δ_l^{CP} for process (1.2) will measure the same combination Γ^{CP} :

$$\delta_l^{CP} = \frac{N_{l+} - N_{l-}}{N_{l+} + N_{l-}} = \frac{\Gamma^{CP}}{\Gamma^{inv}}, \quad (4.9)$$

where $N_{l\pm}$ are the total number of l^\pm in $H^\pm \rightarrow bb'l^\pm\nu$ decay.

For the CP-violating FB asymmetry ΔA^{CP} of the process (1.2) we obtain

$$\Delta A_l^{CP} = 2\alpha_l m_t^2 m_H^2 \frac{m_H^2 - m_t^2}{(m_H^2 + m_t^2)^2} \mathcal{P}^{CP}, \quad (4.10)$$

and the FB asymmetries are at one-loop level

$$A_{l\pm}^{FB} = \beta_t + \alpha_l m_t^2 m_H^2 \frac{(m_H^2 - m_t^2)}{(m_H^2 + m_t^2)^2} (\mathcal{P}^{inv} \pm \mathcal{P}^{CP}). \quad (4.11)$$

Notice, that the only difference between the expressions (3.14) and (4.10) is the coefficient α_b in (3.14) and α_l in (4.10). These coefficients are only connected to the polarization of the t quark. Because of the fact that $\alpha_b = 0.38$ and $\alpha_l = 1$, one would expect a bigger effect measuring (4.10).

5. Numerical Results

Here we present a numerical analysis of the discussed asymmetries. First we analyze the CP-violating asymmetries $\delta_{b,l}^{CP}$, $\Delta A_{b,l}^{CP}$ and ΔR_b^{CP} . Further, we study the FB asymmetries $A_{b,l\pm}^{FB}$ and $R_{b\pm}$ needed for $\Delta A_{b,l}^{CP}$ and ΔR_b^{CP} .

5.1 The CP-violating asymmetries

The expressions \mathcal{P}^{CP} and Γ^{CP} , (2.17) and (3.5), are linear combinations of the CP violating form factors $\text{Re}(\delta Y_t^{CP})$ and $\text{Re}(\delta Y_b^{CP})$. Therefore, we need to measure: 1) the decay rate asymmetries $\delta_{b,l}^{CP}$ which are proportional to Γ^{CP} and 2) the angular and/or energy asymmetries which are proportional to \mathcal{P}^{CP} .

As there is no CP violation in $t \rightarrow bW$, the decay rate asymmetries for (1.1) and (1.2) are equal to the decay rate asymmetry for $H^\pm \rightarrow tb$. We denote it, following ref.[5], by δ^{CP} :

$$\delta^{CP} = \delta_b^{CP} = \delta_l^{CP} = \frac{\Gamma^{CP}}{\Gamma^{inv}}. \quad (5.1)$$

The angular and energy asymmetries are not independent either. As seen from (3.14) and (4.10), the angular asymmetries for leptons and b -quarks are related by:

$$\Delta A_l^{CP} = \frac{\alpha_l}{\alpha_b} \Delta A_b^{CP} \approx 2.6 \Delta A_b^{CP}. \quad (5.2)$$

Further, (3.14) and (3.24) lead to a simple relation between the b -quark energy and angular asymmetries:

$$\Delta R_b^{CP} = \frac{(m_{H^+}^2 + m_t^2)^2}{4m_{H^+}^2 m_t^2} \Delta A_b^{CP}, \quad (5.3)$$

which implies that for $m_{H^+} > m_t$, ΔR_b^{CP} is bigger than ΔA_b^{CP} . Thus, in general, ΔR_b^{CP} is the biggest asymmetry of 2) for $m_{H^+} > 490$ GeV. Fig. 2 illustrates the relative size of the asymmetries $\Delta A_{b,l}^{CP}$ and ΔR_b^{CP} as a function of m_{H^+} . Note that the relations (5.2) and (5.3) are independent of $\tan \beta$.

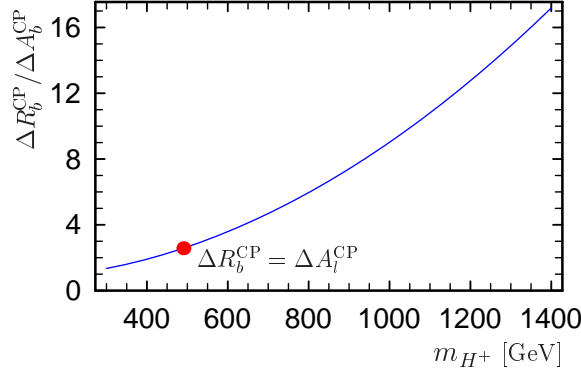


Figure 2: The ratio $\Delta R_b^{CP} / \Delta A_b^{CP}$ as a function of m_{H^+}

Therefore, in the following we shall discuss only the decay rate asymmetry δ^{CP} and the energy asymmetry ΔR_b^{CP} . (Because of a conjugation error in our paper [5] in the formula for the $\tilde{t}\tilde{b}\tilde{g}$ vertex, see the Appendix B, we have redone the numerical analysis for δ^{CP} .) The purpose of our analysis is to determine the size of the asymmetries as functions of m_{H^+} and $\tan \beta$, being the most important parameters of the Higgs sector in MSSM, for different values of the CP-violating phases.

The sources of CP violation in our processes are the one-loop corrections to the H^+tb vertex with intermediate SUSY particles, see Fig. 1a, 1b, 1d, 1e of [5] and the self-energy graph with $\tilde{\tau}\tilde{\nu}_\tau$. (The corrections due to Fig. 1c and Fig. 1f of [5] are of higher order and we do not consider them here.) In order not to deal with too many phases we assume the GUT relation between M_1 and M_2 which fixes $\phi_{M_1} = 0$. According to the experimental limits on the electric and neutron EDM's, we take $\phi_\mu = 0$ or $\phi_\mu = \pi/10$. Thus, the remaining CP-violating phases in our study are the phases of A_t , A_b and A_τ which we shall vary. If not specified otherwise, we fix the following values for the other MSSM parameters:

$$M_2 = 300 \text{ GeV}, \quad M_3 = 745 \text{ GeV}, \quad M_{\tilde{U}} = M_{\tilde{Q}} = M_{\tilde{D}} = M_E = M_L = 350 \text{ GeV},$$

$\tan \beta$	$m_{\tilde{\chi}_1^0}$	$m_{\tilde{\chi}_2^0}$	$m_{\tilde{\chi}_3^0}$	$m_{\tilde{\chi}_4^0}$	$m_{\tilde{\chi}_1^+}$	$m_{\tilde{\chi}_2^+}$	$m_{\tilde{t}_1}$	$m_{\tilde{t}_2}$	$m_{\tilde{b}_1}$	$m_{\tilde{b}_2}$	$m_{\tilde{\tau}_1}$	$m_{\tilde{\tau}_2}$	$m_{\tilde{\nu}}$
5	142	300	706	706	300	709	166	522	327	377	344	362	344
30	141	296	705	709	296	711	172	519	183	464	295	402	344

Table 1: Masses of the sparticles (in GeV) for the parameter set (5.4) together with $\phi_{A_t} = \phi_{A_b} = \pi/2$ and $\phi_\mu = 0$.

$$\mu = -700 \text{ GeV}, \quad |A_t| = |A_b| = |A_\tau| = 700 \text{ GeV} \quad (5.4)$$

The relevant masses of the sparticles for the choice (5.4) and $\tan \beta = 5$ or 30 are given in Table 1. For the case with $\phi_\mu = \pi/10$ and the other parameters unchanged, all masses do not change by more than 1 GeV from those given in Table 1, except for $m_{\tilde{t}_1} = 187$ GeV and $m_{\tilde{t}_2} = 515$ GeV for $\tan \beta = 5$, and $m_{\tilde{t}_1} = 176$ GeV for $\tan \beta = 30$. Note that $\phi_\mu = \pi/10$ implies $\mu = -700 e^{i\pi/10}$ GeV. We have used running top and bottom Yukawa couplings, calculated at the scale $Q = m_{H^+}$, see Appendix A. We have checked that the asymmetries have only a very weak dependence on the scale Q .

Fig. 3 shows the asymmetries δ^{CP} and ΔR_b^{CP} as functions of m_{H^+} for $\phi_{A_t} = \pi/2$, $\phi_{A_b} = 0$ and $\phi_\mu = 0$. As one can see, for $\tan \beta = 5$ the decay rate asymmetry δ^{CP} goes up to 20%, while ΔR_b^{CP} reaches 8% for the same values of the parameters. The asymmetries strongly depend on $\tan \beta$ and they quickly decrease as $\tan \beta$ increases. Our studies have

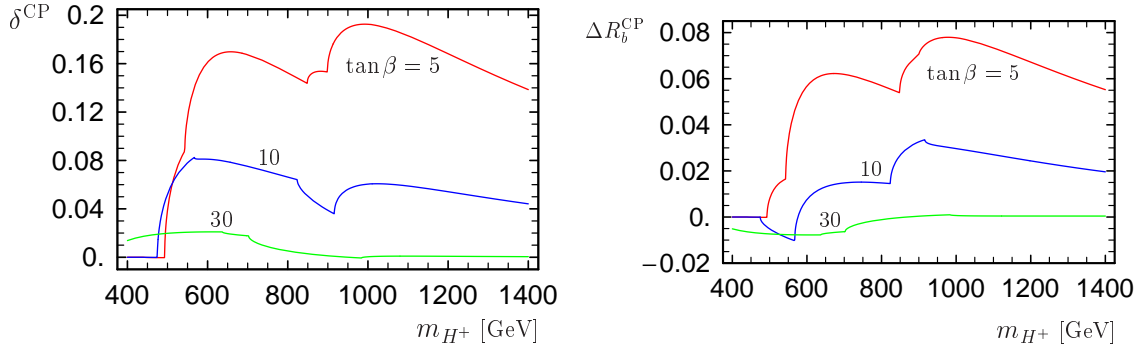


Figure 3: The asymmetries δ^{CP} and ΔR_b^{CP} as a function of m_{H^+} for $\phi_{A_t} = \pi/2$, $\phi_{A_b} = \phi_\mu = 0$. The red, blue, and green lines are for $\tan \beta = 5, 10$, and 30.

shown that the most important CP-violating phase is ϕ_{A_t} . There is only a very weak dependence on ϕ_{A_b} and ϕ_{A_τ} . We therefore take them zero.

The main contributions to both δ^{CP} and ΔR_b^{CP} come from the self-energy graph with stop-sbottom. The vertex graph with stop-sbottom-gluino also gives a non-zero contribution. Their contributions are shown in Fig. 4. The contribution of the rest of the graphs is negligible. This justifies the use of the GUT relation which fixes $\phi_{M_1} = 0$, and it explains the weak dependence on ϕ_{A_τ} .

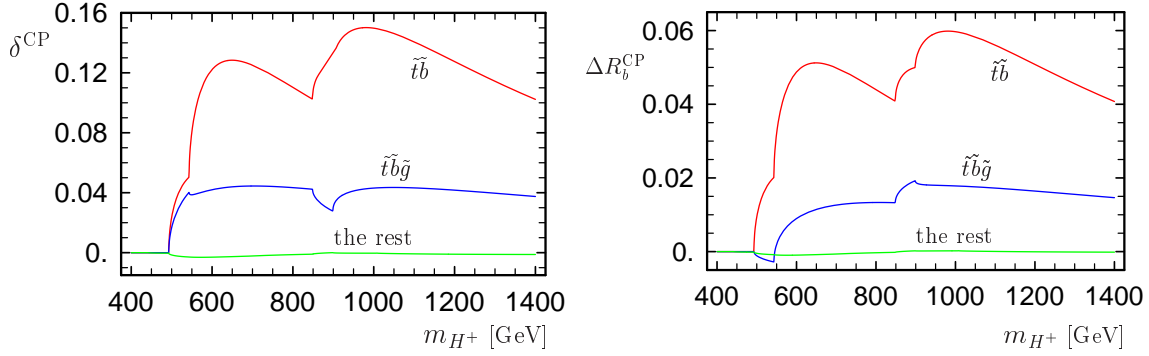


Figure 4: The contribution of the $\tilde{t}\tilde{b}$ self-energy (red line), $\tilde{t}\tilde{b}\tilde{g}$ vertex contribution (blue line) and the sum of the other (green line) diagrams to δ^{CP} and ΔR_b^{CP} as a function of m_{H^+} for $\tan\beta = 5$ and $\phi_{A_t} = \pi/2$, $\phi_{A_b} = \phi_\mu = 0$.

Up to now, all the analyses are done for $M_3 = m_{\tilde{g}} = 744$ GeV. In Fig. 5, we show the dependence of δ^{CP} on the gluino mass. In general, δ^{CP} gets small with increasing gluino mass.

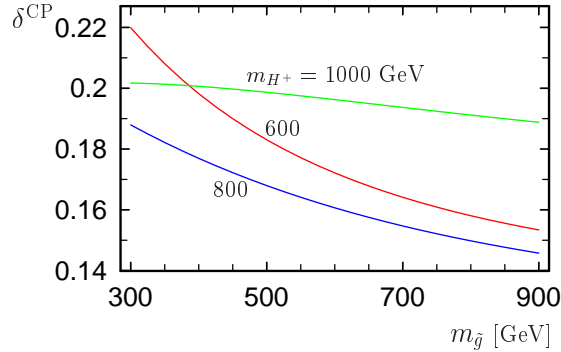


Figure 5: δ^{CP} as a function of the gluino mass for $\tan\beta = 5$. The red line is for $m_{H^+} = 600$ GeV, the blue line is for $m_{H^+} = 800$ GeV and the green line is for $m_{H^+} = 1000$ GeV.

Let us now allow a non-zero phase of μ . We take a very small phase, $\phi_\mu = \pi/10$, in order not to be in contradiction with the experimental data. As can be seen in Fig. 6, the asymmetries can increase up to 25% for δ^{CP} and 10% for ΔR_b^{CP} . The discussed asymmetries δ^{CP} and ΔR_b^{CP} show a very strong dependence on the sign of μ . As noted above, our analysis is done for $\mu = -700$ (see (5.4)), however if μ changes sign, $\mu = 700$, all asymmetries become extremely small.

5.2 The P-violating asymmetries

When discussing the possibilities to measure $\Delta A_{b,l}^{CP}$ and ΔR_b^{CP} , it is also important to know the size of the FB asymmetries $A_{b,l\pm}^{FB}$, (3.17) and (4.11), and of the energy asymmetry $R_{b\pm}$, (3.23), that enter the corresponding CP-violating asymmetries.

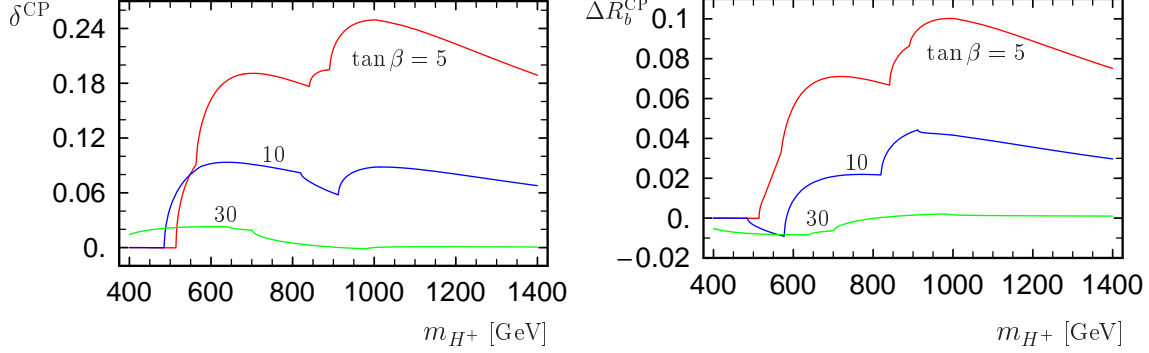


Figure 6: The asymmetries δ^{CP} and ΔR_b^{CP} as a function of m_{H^+} for $\phi_{A_t} = \pi/2$, $\phi_{A_b} = 0$ and a non zero phase of μ , $\phi_\mu = \pi/10$. The red, blue and green lines are for $\tan \beta = 5, 10$, and 30 .

$A_{b,l\pm}^{FB}$ and $R_{b\pm}$ are determined by the polarization \mathcal{P}^\pm of the t -quark in $H^\pm \rightarrow tb$ decays. As the Lagrangian violates parity, these asymmetries appear already at tree level and thus should be rather large.

Neglecting the loop induced CP-violating part \mathcal{P}^{CP} in (3.17), (4.11), and (3.23), we get

$$A_{b,l}^{inv} = \frac{1}{2} (A_{b,l+}^{FB} + A_{b,l-}^{FB}) = \beta_t + \alpha_{b,l} m_t^2 m_{H^+}^2 \frac{(m_{H^+}^2 - m_t^2)}{(m_{H^+}^2 + m_t^2)^2} \mathcal{P}^{inv}, \quad (5.5)$$

$$R_b^{inv} = \frac{1}{2} (R_{b+} + R_{b-}) = \frac{1}{4} \alpha_b (m_{H^+}^2 - m_t^2) \mathcal{P}^{inv} \simeq \frac{\alpha_b}{2} \frac{y_t^2 - y_b^2}{y_t^2 + y_b^2}. \quad (5.6)$$

Thus $\Delta A_{b,l}^{CP}$, (3.14, 4.10), and ΔR_b^{CP} , (4.10), are determined by \mathcal{P}^{CP} , while $A_{b,l}^{FB}$ and R_b are determined by \mathcal{P}^{inv} , and there is no a priori reason to expect that their $\tan \beta$ and m_{H^+} dependences will be the same. $A_{b,l}^{inv}$ and R_b^{inv} are tree-level quantities. Including the one-loop corrections to these would require the full renormalization of the process which is beyond the scope of this paper.

In Fig. 7 we present A_b^{inv} and A_l^{inv} as a function of m_{H^+} for $\tan \beta = 5, 10$, and 30 , and in Fig. 8 we show R_b^{inv} as a function of $\tan \beta$. Note that at tree-level $A_{b,l}^{FB}$ depends only on $\tan \beta$ and m_{H^+} , and R_b only on $\tan \beta$.

6. Conclusions

We have calculated the CP-violating decay rate, forward-backward and energy asymmetries between $H^+ \rightarrow \bar{b}t \rightarrow \bar{b}b'W^+(\rightarrow \bar{b}b'l^+\nu_l)$ and $H^- \rightarrow b\bar{t} \rightarrow b\bar{b}'W^-(\rightarrow b\bar{b}'l^-\nu_l)$. They are induced by loop corrections in the $H^\pm tb$ - vertex. The CP violating forward-backward and energy asymmetries are determined by the polarization of the top quark and are therefore related. We have shown that it is necessary to measure *both* the decay rate asymmetry δ^{CP} and the forward-backward or the energy asymmetry to get the maximal information on the CP-violating parts of the decay amplitude. We have performed a detailed numerical

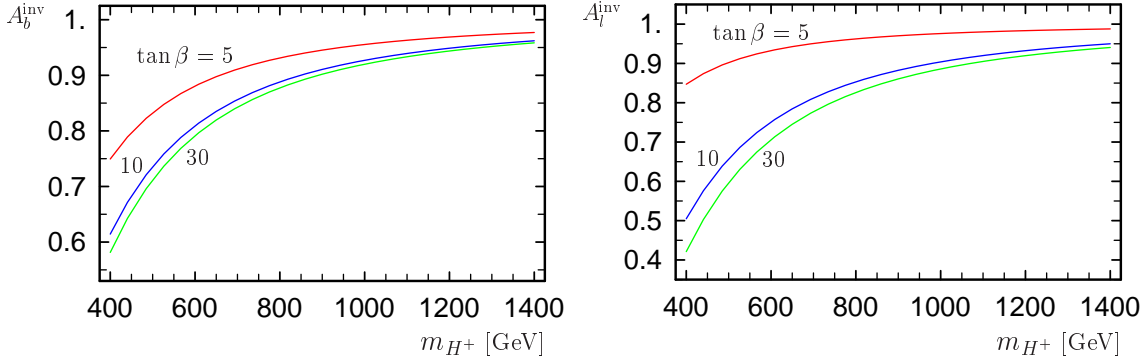


Figure 7: The forward-backward asymmetries A_b^{inv} and A_l^{inv} as a function of m_{H^+} for $\tan \beta = 5$ (red), 10 (blue), and 30 (green).

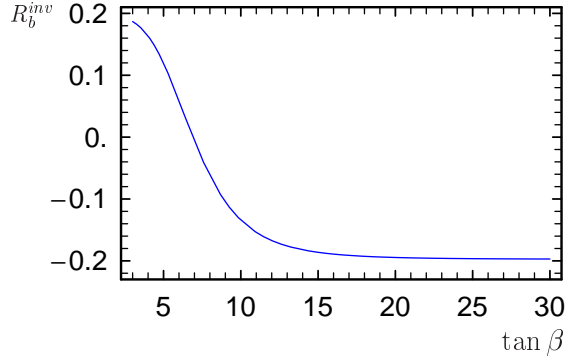


Figure 8: The energy asymmetry R_b^{inv} as a function of $\tan \beta$

analysis of these quantities. An important improvement with running Yukawa couplings at the m_{H^+} scale has been made. The asymmetries are most sensitive to the phase ϕ_{A_t} . The asymmetries reach their maximum for $\tan \beta = 5$ and $\mu = -700$ GeV. The decay rate asymmetry can go up to 25%, the others up to 10%. The main contribution comes from the self-energy diagram with stop and sbottom exchange. We have also calculated the P-violating asymmetries at tree level.

We want to add a few remarks on the measurability of these asymmetries. In principle, the production rate for H^\pm at LHC is not so small being 0.2 pb for $m_{H^+} = 500$ GeV and $\tan \beta = 30$ [10, 11]. The main production process is due to $g \bar{b} \rightarrow H^+ \bar{t}$. Because of the large background, the actual signal production rate is strongly reduced. According to [10], one can expect $N = 733$ signals with $N/\sqrt{B} = 12.6$ for $m_{H^+} = 500$ GeV, $\tan \beta = 50$ for a luminosity $\mathcal{L} = 100 \text{ fb}^{-1}$. The statistical significance $\sqrt{N} A$ to measure an asymmetry A of several percent might be too low for a clear observation of CP violation in H^+ decays at LHC in the first stage. However, at SLHC for which a luminosity of 1000-3000 fb^{-1} is designed, such a measurement would be worth of being performed. Here we have only considered CP violation in the H^+ decays. However, similar graphs are also present in the production process $g \bar{b} \rightarrow H^+ \bar{t}$ [8]. One would expect a CP-violating asymmetry

of similar size. The total asymmetry in production and decay would be approximately additive, $A_{\text{tot.}} = A_{\text{prod.}} + A_{\text{decay}}$.

Acknowledgements

We thank Jennifer Williams for finding the conjugation error in [5]. The authors acknowledge support from EU under the MRTN-CT-2006-035505 network programme. This work is supported by the "Fonds zur Förderung der wissenschaftlichen Forschung" of Austria, project No. P18959-N16.

A. Running Yukawa couplings

For clarity, we present all formulas used for programming the running top and bottom Yukawa couplings, h_b and h_t , respectively. The Lagrangian for the $H^\pm tb$ interactions reads

$$\mathcal{L}_{Hqq} = H^+ \bar{t} (y_b^* P_R + y_t P_L) b + H^- \bar{b} (y_t^* P_R + y_b P_L) t + \dots, \quad (\text{A.1})$$

with the $\overline{\text{DR}}$ running top and bottom Yukawa couplings in the MSSM,

$$y_b = h_b \sin \beta, \quad y_t = h_t \cos \beta, \quad (\text{A.2})$$

given at the scale $Q = m_{H^+}$ in our studied case, and

$$h_b = \frac{gm_b^{\overline{\text{DR}}}(Q)}{\sqrt{2}m_W \cos \beta}, \quad h_t = \frac{gm_t^{\overline{\text{DR}}}(Q)}{\sqrt{2}m_W \sin \beta}. \quad (\text{A.3})$$

In [4] it is shown that within an effective theory approach large finite scale independent parts can be resummed, which in case of complex MSSM input parameters leads to complex h_b and h_t . Effective means that the masses of the particles in the loops are much bigger than those of the in- and outgoing particles so that these states can be integrated out in the Lagrangian. In our case, we are interested in additional open channels, e. g. $H^+ \rightarrow t\tilde{b}$. This implies that the resummation is not applicable here. But we can improve our calculation by using full one-loop running quark masses with some higher order improvements of the gluonic part. Note, that $m_q^{\overline{\text{DR}}}(Q)$ can always be made real by field redefinition [4] and therefore also h_q is real in our case.

We take as input set the bottom mass $m_b^{\overline{\text{MS}}}(m_b) = 4.2$ GeV, the mass for the top quark is the pole mass, $m_t^{\text{pole}} = 171.4$ GeV, the strong coupling is $\alpha_s^{\overline{\text{MS}}}(m_Z) = 0.1176$, $m_Z = 91.1876$ GeV, and $m_W = 80.406$ GeV

First we want to have the $\overline{\text{DR}}$ bottom mass of the Standard Model at the scale Q (see for comparison eq. (26) in [13]),

$$m_{b,\text{SM}}^{\overline{\text{DR}}}(Q) = m_b^{\overline{\text{MS}}}(Q) \left[1 - \frac{\alpha_s^{\overline{\text{DR}}}}{3\pi} - \frac{23\alpha_s^{2,\overline{\text{DR}}}}{72\pi} \right] \quad (\text{A.4})$$

with $m_b^{\overline{\text{MS}}}(Q) \equiv m_b(Q)_{\text{SM}}$ given in [14, 15]. Adding the loop contributions due to supersymmetric and heavy SM particles, denoted by $\Delta m_b^{\text{extra}}$ (calculated in the $\overline{\text{DR}}$ renormalization scheme), we get the full one-loop $\overline{\text{DR}}$ running bottom mass (with some higher-order improvements) within the MSSM,

$$m_b^{\overline{\text{DR}}}(Q) = m_{b,\text{SM}}^{\overline{\text{DR}}}(Q) + \Delta m_b^{\text{extra}}(Q). \quad (\text{A.5})$$

The $\overline{\text{DR}}$ running top mass we get from

$$m_t^{\overline{\text{DR}}}(Q) = m_t^{\text{pole}} \left[1 + \frac{\Delta m_t^{(1)}}{m_t} + \frac{\Delta m_t^{(2,g)}}{m_t} \right] \quad (\text{A.6})$$

where $\Delta m_t^{(1)}$ is the full one-loop contribution to m_t (calculated in the $\overline{\text{DR}}$ renormalization scheme) and $\Delta m_t^{(2,g)}$ is the gluonic two-loop contribution,

$$\frac{\Delta m_t^{(2,g)}}{m_t} = - \left(\frac{\alpha_s(Q)}{4\pi} \right)^2 \left(\frac{8\pi^2}{9} + \frac{2011}{18} + \frac{16\pi^2 \log(2)}{9} - \frac{8\xi(3)}{3} + 82L + 22L^2 \right), \quad (\text{A.7})$$

with $L = \log(Q^2/m_t^2)$, see [16].

B. Squark–quark–gluino contribution

In Appendix B of [5], eq. (62) is incorrect and therefore also eqs. (14, 15). For clarification, the definition of the squark rotation matrix $R^{\tilde{q}}$ is essential. In this work and in [5], one has

$$\tilde{q}_\alpha = R_{i\alpha}^* \tilde{q}_i \quad \text{with} \quad \alpha = L, R \quad \text{and} \quad i = 1, 2. \quad (\text{B.1})$$

Hence, the squark–quark–gluino interaction (eq. (62) of [5]) is given by

$$\begin{aligned} \mathcal{L}_{q\tilde{q}\tilde{g}} = & -\sqrt{2} g_s T_{st}^a \left[\bar{\tilde{g}}^a (R_{1i}^{\tilde{q}*} e^{-\frac{i}{2}\phi_3} P_L - R_{2i}^{\tilde{q}*} e^{\frac{i}{2}\phi_3} P_R) q_s \tilde{q}_{i,t}^* \right. \\ & \left. + \bar{q}_s (R_{1i}^{\tilde{q}} e^{\frac{i}{2}\phi_3} P_R - R_{2i}^{\tilde{q}} e^{-\frac{i}{2}\phi_3} P_L) \tilde{g}^a \tilde{q}_{i,t} \right], \end{aligned} \quad (\text{B.2})$$

The contribution from the diagram with a stop, a sbottom, and a gluino (in [5] eqs. (14,15)) is

$$\begin{aligned} \text{Re } \delta Y_b^{CP}(\tilde{t}_i \tilde{b}_j \tilde{g}) = & -\frac{4}{3} \frac{\alpha_s}{\pi} [m_{\tilde{g}} \text{Im}(G_{4ij} R_{1i}^{\tilde{t}} R_{2j}^{\tilde{b}*} e^{i\phi_3}) \text{Im}(C_0) \\ & + m_t \text{Im}(G_{4ij} R_{2i}^{\tilde{t}} R_{2j}^{\tilde{b}*}) \text{Im}(C_1) + m_b \text{Im}(G_{4ij} R_{1i}^{\tilde{t}} R_{1j}^{\tilde{b}*}) \text{Im}(C_2)], \end{aligned} \quad (\text{B.3})$$

$$\begin{aligned} \text{Re } \delta Y_t^{CP}(\tilde{t}_i \tilde{b}_j \tilde{g}) = & -\frac{4}{3} \frac{\alpha_s}{\pi} [m_{\tilde{g}} \text{Im}(G_{4ij} R_{2i}^{\tilde{t}} R_{1j}^{\tilde{b}*} e^{-i\phi_3}) \text{Im}(C_0) \\ & + m_t \text{Im}(G_{4ij} R_{1i}^{\tilde{t}} R_{1j}^{\tilde{b}*}) \text{Im}(C_1) + m_b \text{Im}(G_{4ij} R_{2i}^{\tilde{t}} R_{2j}^{\tilde{b}*}) \text{Im}(C_2)], \end{aligned} \quad (\text{B.4})$$

with $C_X = C_X(m_t^2, m_{H^+}^2, m_b^2, m_{\tilde{g}}^2, m_{\tilde{t}_i}^2, m_{\tilde{b}_j}^2)$.

References

- [1] P. Nath, Phys.Rev. Lett. **66** (1991) 2565; Y. Kizukuri and N. Oshimo, Phys. Rev. **D 46** (1992) 3025; R. Garisto and J. D. Wells, Phys. Rev. **D 55** (1997) 1611 [hep-ph/9609511]; Y. Grossman, Y. Nir and R. Rattazzi, Adv. Ser. Direct. High Energy Phys. **15** (1998) 755 [hep-ph/9701231].
- [2] T. Ibrahim and P. Nath, Phys. Lett. **B 418** (1998) 98 [hep-ph/9707409]; M. Brhlik, G. J. Good and G. L. Kane, Phys. Rev. **D 59** (1999) 115004 [hep-ph/9810457]; A. Bartl, T. Gajdosik, W. Porod, P. Stöckinger and H. Stremnitzer, Phys. Rev. **D 60** (1999) 073003 [hep-ph/9903402].
- [3] A. Pilaftsis, Phys. Rev. **D 58** (1998) 096010 [hep-ph/9805373] and Phys. Lett. **B 435** (1998) 88 [hep-ph/9805373]; A. Pilaftsis and C. E. Wagner, Nucl. Phys. **B 553** (1999) 3 [hep-ph/9902371]; D. A. Demir, Phys. Rev. **D 60** (1999) 055006 [hep-ph/9901389].
- [4] M. Carena, J. R. Ellis, A. Pilaftsis and C. E. Wagner, Nucl. Phys. **B 586** (2000) 92 [hep-ph/0003180].
- [5] E. Christova, H. Eberl, S. Kraml and W. Majerotto, Nucl. Phys. **B 639** (2002) 263 [hep-ph/0205227]; Erratum-ibid. **B 647** (2002) 359.
- [6] E. Christova, H. Eberl, S. Kraml and W. Majerotto, JHEP **0212** (2002) 021 [hep-ph/0211063].
- [7] E. Christova, E. Ginina, M. Stoilov JHEP **11** (2003) 027 [hep-ph/0307319].
- [8] J. Williams, contribution to CPNSH Report, CERN-2006-009 [hep-ph/0608079].
- [9] S. M. Bilenky, E. Christova, N. Nedelcheva, Bulg. J. Phys. **13** (1986) 283
S. M. Bilenky, Introduction to the Physics of Electroweak Interactions (Pergamon, Oxford 1992).
- [10] A. Belyaev, D. Garcia, J. Guasch, J. Sola, JHEP **0206** (2002) 059 [hep-ph/0203031].
- [11] V. D. Barger, R. J. N. Phillips, D. P. Roy, Phys. Lett. **B 324** (1994) 236 [hep-ph/9311372]; J. Alwall, J. Rathsmann, JHEP **50** (2004) 050 [hep-ph/0409094]; E. L. Berger, T. Han, J. Jiang, T. Plehn, Phys. Rev. **D 71** (2005) [hep-ph/0312286].
- [12] J. A. Aguilar-Saavedra et al., EPJ **C 46** (2006) 43 [hep-ph/0511344].
- [13] J. A. Aguilar-Saavedra et al., EPJ **C 46** (2006) 43 [hep-ph/0511344].
- [14] H. Eberl, K. Hidaka, S. Kraml, W. Majerotto, Y. Yamada, Phys. Rev. **D 62** (2000) 055006, [hep-ph/9912463].
- [15] S.G. Gorishny, A.L. Kataev, S.A. Larin, and L.R. Surguladze, Mod. Phys. Lett. **A5** (1990) 2703; Phys. Rev. **D 43** (1991) 1633;
A. Djouadi, M. Spira, and P.M. Zerwas, Z. Phys. **C 70** (1996) 427;
A. Djouadi, J. Kalinowski, and M. Spira, Comput. Phys. Commun. **108** (1998) 56;
M. Spira, Fortschr. Phys. **46** (1998) 203.
- [16] A. Bednyakov, A. Onishchenko, V. Velizhanin, O. Veretin, Eur. Phys. J. **C 29** (2003) 87, [hep-ph/0210258].